1 One-dimensional optical lattice potential

The contents of this section follow the derivation found in Sec. IV A of [1].

The hamiltonian for an atom moving in a 1D lattice potential is

$$H_{\text{single,1D}} = -\frac{\hbar^2}{2m}\frac{\partial^2}{\partial x^2} + V_0 \sin^2(kx) \tag{1}$$

where $k = 2\pi/\lambda$, and λ is the wavelength of the lattice laser. The lattice spacing is $a = \lambda/2$. If V_0 is in units of the recoil energy $E_R = \frac{\hbar^2 k^2}{2m}$, then the hamiltonian can be written as

$$\begin{aligned} H_{\text{single,1D}} &= -\frac{1}{k^2}\frac{\partial^2}{\partial x^2} + V_0 \sin^2(kx) \\ H_{\text{single,1D}} &= -\frac{1}{k^2}\frac{\partial^2}{\partial x^2} + \frac{V_0}{4}(2 - e^{2ikx} - e^{-2ikx}) \end{aligned} \tag{2}$$

The solution to this equation can be found in terms of Bloch states, which are labeled by their quasi-momentum q, and their band index n

$$\psi_q^n(x) = e^{iqx} \sum_{m\in\mathbb{Z}} c_{qm}^n e^{imGx} \tag{3}$$

The lattice translation invariant function that typically accompanies e^{iqx} has been written here as a sum of plane waves (labeled by the integer m) at the reciprocal lattice vectors. This is the Fourier series of any such periodic function and represents no loss of generality. The reciprocal lattice vector $G = \frac{2\pi}{a} = 2k$, where $a = \lambda/2$ is the lattice spacing.

Plugging the Bloch states into the hamiltonian and then rearranging some of the terms in the infinite sum, we get

$$\begin{aligned} H_{\text{single,1D}}\psi_q(x) &= \sum_m \left[(q/k + 2m)^2 + \frac{V_0}{4}(2 - e^{2ikx} - e^{-2ikx})\right] c_{qm}^n e^{iqx + im2kx} \\ H_{\text{single,1D}}\psi_q(x) &= \sum_m \left[\left((q/k + 2m)^2 + \frac{V_0}{2}\right) c_{qm}^n - \frac{V_0}{4}c_{q,m-1}^n - \frac{V_0}{4}c_{q,m+1}^n\right] e^{iqx + im2kx} \end{aligned} \tag{4}$$

The left hand side of the time-independent Schrodinger equation is simply

$$E_q^n \psi_q(x) = \sum_m E_q c_{qm}^n e^{iqx + imGx} \tag{5}$$

For the coefficients c_{qm}^n to represent an eigenstate of the problem, the Bloch state needs to satisfy $H\psi_q(x) = E_q^n \psi_q(x)$, and since the plane waves are linearly independent functions this means that

$$\left((q/k + 2m)^2 + \frac{V_0}{2}\right) c_{qm}^n - \frac{V_0}{4}c_{q,m-1}^n - \frac{V_0}{4}c_{q,m+1}^n = E_q c_{qm}^n \tag{6}$$

The quasimomentum is restricted to the first Brillouin zone, which can be taken to be between $[-\frac{\pi}{a}, \frac{\pi}{a})$ or between $[0, \frac{2\pi}{a})$. We will express the quasimomentum in units of $\frac{2\pi}{a} = 2\pi$, so in the equation above we will make the replacement $q/k \to 2q$. Also in the equation for the Bloch state $q \to 2\pi q$

We then have a linear system of equations which determines the c_{qm}^n. The number of equations is infinite, but for our practical purposes we will truncate it such that $|m| < \mathcal{N}$. The resulting equations

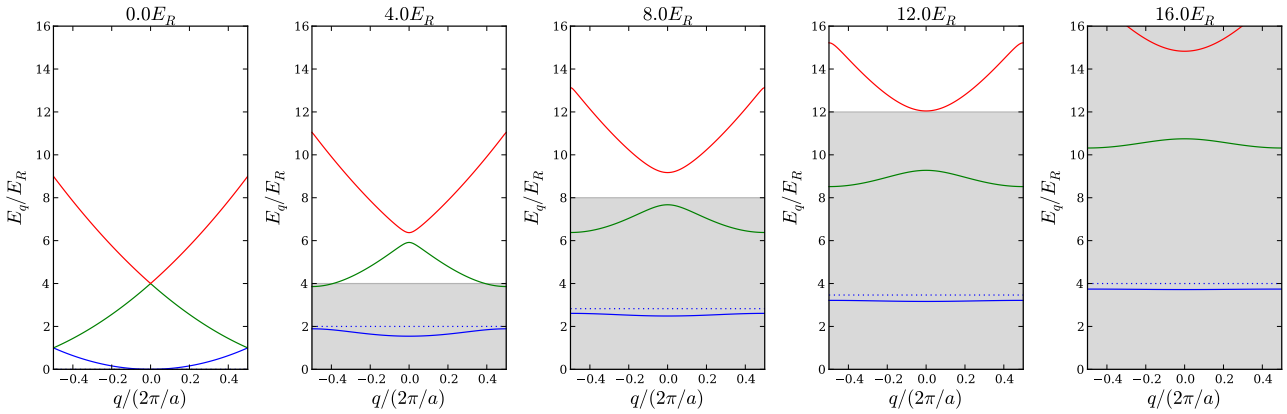

Figure 1: Band structure in a 1D optical lattice. The depth of the lattice is indicated by the shaded area, and the energy of the hamonic oscillator ground state in a single lattice site is shown as a dotted line.

can be written in matrix form, for example if we select $\mathcal{N} = 2$

$$\begin{bmatrix} \frac{1}{2}V_0+4(q-2)^2 & -\frac{1}{4}V_0 & 0 & 0 & 0 \\ -\frac{1}{4}V_0 & \frac{1}{2}V_0+4(q-1)^2 & -\frac{1}{4}V_0 & 0 & 0 \\ 0 & -\frac{1}{4}V_0 & \frac{1}{2}V_0+4q^2 & -\frac{1}{4}V_0 & 0 \\ 0 & 0 & -\frac{1}{4}V_0 & \frac{1}{2}V_0+4(q+1)^2 & -\frac{1}{4}V_0 \\ 0 & 0 & 0 & -\frac{1}{4}V_0 & \frac{1}{2}V_0+4(q+2)^2 \end{bmatrix} \tag{7}$$

In the numerical solution that we implemented we chose $\mathcal{N} = 5$, it turns out that to accurately obtain the dispersion relationship for the n^{th} band you pretty much only need $\mathcal{N} = n + 1$, so using $\mathcal{N} = 5$ is somewhat overkill for us since we will be mostly concentrated on the lowest band and the first excited band.

1.1 Band structure

We can find the solutions for the set of coefficients c^n_{qm} by diagonalizing the matrix shown above. The eigenvalues correspond to the energies E^n_q as a function of quasimomentum q and band index n, this set of solutions is referred to as the band structure, and we show it for a 1D lattice as a function of q in Fig. 1, and also as a function of lattice depth in Fig. 2

We mention here that the Schrodinger equation for the hamiltonian in Eq. 1, has solutions called Mathieu functions. One can calculate the band structure by using the known properties of the Mathieu functions, which are avaiable on tables or as functions in some softare packages (e.g. Mathematica), see for instance the treatement in [2].

1.2 Eigenstates

For each energy eigenvalue we have an associated eigenstate which is defined in terms of the c^n_{qm} by Eq. 3. Typically, numerical diagonalization routines return the normalized eigenvectors of the matrix in question, and for us this means that the coefficients c^n_{qm} will satisfy

$$\sum_m |c^n_{qm}|^2 = 1 \tag{8}$$

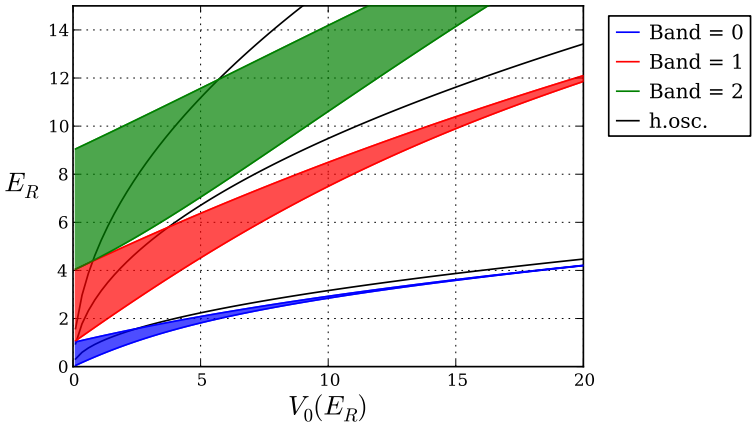

Figure 2: Band structure in a 1D optical lattice. Each band is indicated by the colored area, the harmonic oscillator states in an isolated lattice site are shown as black lines.

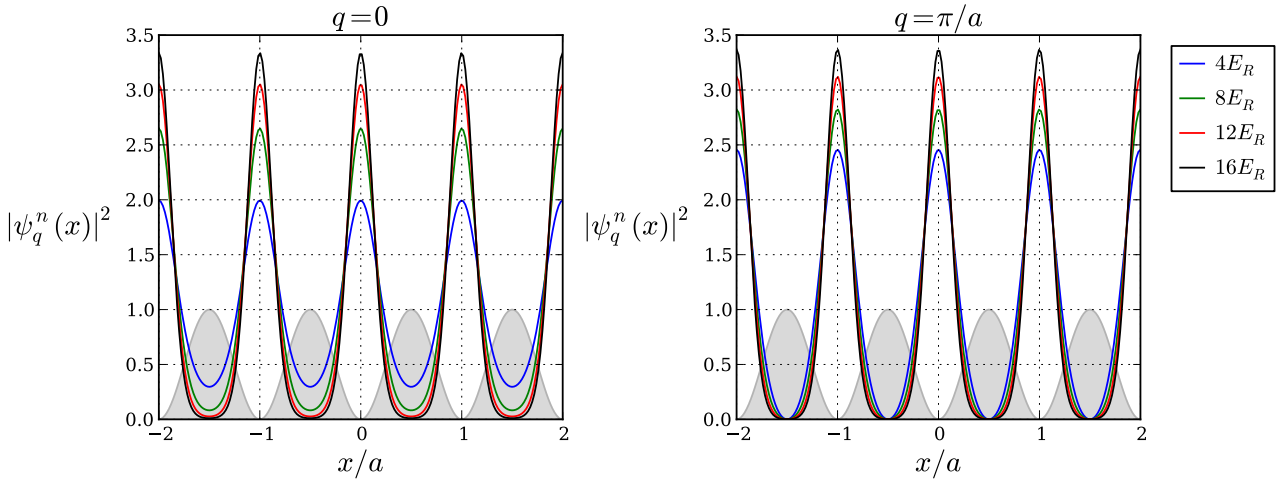

Figure 3: Eigenstates of the Hamiltonian in a 1D optical lattice shown for $q = 0$ (left) and $q = \pi/a$ (right) for various lattice depths. The states are normalized so that the integral of the probability density over one lattice site is equal to one. The gray shaded region is shown to indicate the variation of the lattice potential.

This has the implication that the states obtained from Eq. 3 will be normalized over a lattice site. In Fig. 3. we show the probability density for a lowest band eigenstate as a function of position in the lattice for various lattice depths. One can see how, as the lattice gets deeper, the state becomes more localized around the center of each lattice site.

1.3 Wannier states

It is useful to define a basis of states that are localized around a single lattice site. We will see later on that when using such a basis the hamiltonian for the Hubbard model takes its most familiar form. The localized states, centered around the site at x_j, can be constructed as the following superposition

of eigenstates of the hamiltonian [1]

$$w^n(x - x_j) = \frac{1}{L} \sum_q e^{-iq2\pi x_j} \psi_q^n(x) \tag{9}$$

Here we have considered a finite sized lattice with a total of L sites. We use the set of unique quasi-momenta defined by $q = \frac{2\pi n}{a}$ $\forall n \in \{0, 1, \dots L-1\}$. The definition of this set is arbitrary, but there is no loss of generality. This becomes clear we insert the expansion of $\psi_q^n(x)$ in plane waves into the definition of the Wannier state.

$$w^n(x - x_j) \equiv w_j^n(x) = \frac{1}{L} \sum_q \sum_{m \in \mathbb{Z}} c_{qm}^n e^{-i2\pi q x_j} e^{i2\pi(q+m)x} \tag{10}$$

The Wannier state is a sum of plane waves, and all plane waves will be covered, regardless of the set of unique quasimomenta that we decide to consider, since m runs over all integers. We will set $x_j = 0$ for the calculation of the Wannier function. WWannier states centered at different lattice sites can be obtained by translation of the $x_j = 0$ solution.

$$w_0^n(x) = \frac{1}{L} \sum_q \sum_{m \in \mathbb{Z}} c_{qm}^n e^{i2\pi(q+m)x} \tag{11}$$

Since the hamiltonian communtes with the parity operator it is required that $\psi_q^n(-x) = \pm\psi_q^n(x)$ which implies that $c_{qm}^n = \pm c_{q'm'}^n$ if $(q+m) = -(q'+m')$. Then, the Wannier state becomes

$$w_0^n(x) = \frac{1}{L} \left(c_{00}^n + \sum_{q>0} \sum_{m>0} c_{qm}^n \left[e^{i2\pi(q+m)x} \pm e^{-i2\pi(q+m)x} \right] \right) \tag{12}$$

It is shown in [4] that the maximally localized Wannier states are obtained if the plus sign is chosen for even bands and the minus sing is chosen for odd bands. So, the Wannier states are symmetric for the even bands and antisymmetric for the odd bands.

$$w_0^n(x) = \frac{c_{00}^n}{L} + \frac{2}{L} \sum_{q>0} \sum_{m>0} c_{qm}^n \begin{cases} \cos[2\pi(q+m)x] & \text{if } n \text{ even} \\ \sin[2\pi(q+m)x] & \text{if } n \text{ odd} \end{cases} \tag{13}$$

For $q, m > 0$ all the coefficients c_{qm}^n will have the same sign, so we select them to be positive.

We can now proceed to add up the plane waves to obtain the Wannier states which are shown in Fig. 4 for various lattice depths. As the lattice depth is increased, the Wannier states become more localized. This leads to less overlap betweeen Wannier states in adjacent sites, which results in a reduction of the amplitude for a particle to tunnel from one site to the next one. More localized states also imply that the on-site interaction will be larger, since two particles in the same site will be closer to each other on average.

In Fig. 5 we show the Wannier functions for the first three bands in a $4E_R$ lattice.

2 Three-dimensional optical lattice potential

The hamiltonian for an atom moving in a 3D lattice can be separated in the three spatial coordinates. So we can use the solutions that were obtained in the previous section for the 1D lattice and obtain the band structure and the Wannier states for the 3D lattice. The band structure is shown in Fig. 6.

[1] In some treatments (for instance [3]) the Wannier function is defined with a normalization factor of $\sqrt{N_s}$ rather than N_s as shown here. This is considering eigenfunctions $\psi_q^n(x)$ which are normalized when integrating over the full extent in the lattice. We stick to the N_s normalization factor, without the square root, since the eigenfunctions that are obtained numerically come out normalized over a lattice site, as was explained in the previous section.

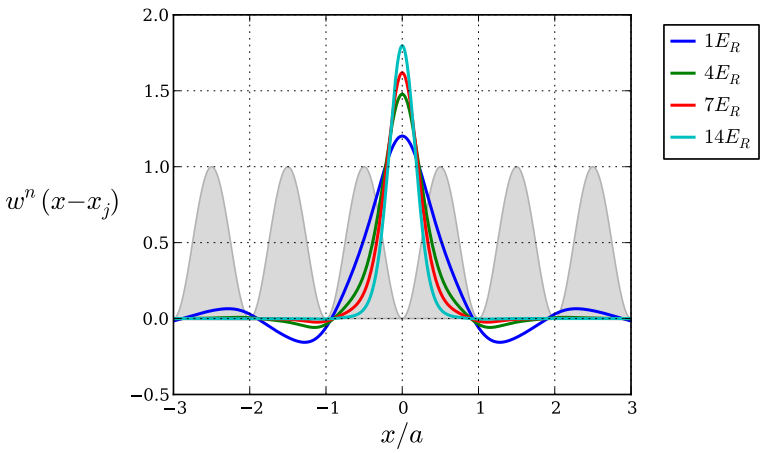

Figure 4: Localized Wannier states in a 1D optical lattice for various lattice depths. The gray shaded region is shown to indicate the spatial variation of the lattice potential.

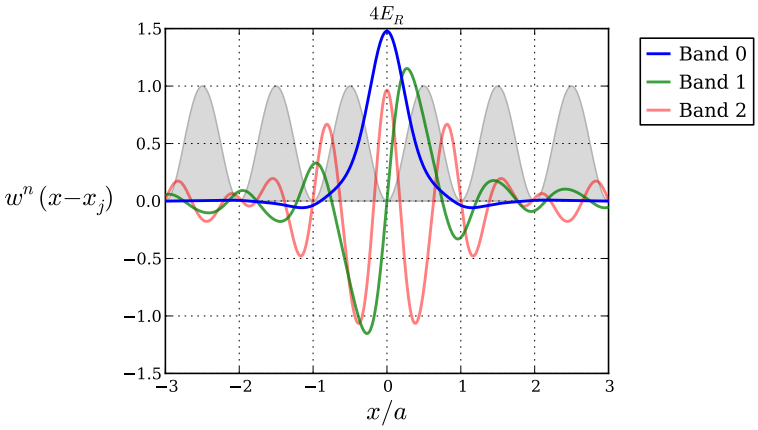

Figure 5: Localized Wannier states in a $4E_R$ 1D optical lattice for the first three energy bands. The gray shaded region is shown to indicate the spatial variation of the lattice potential.

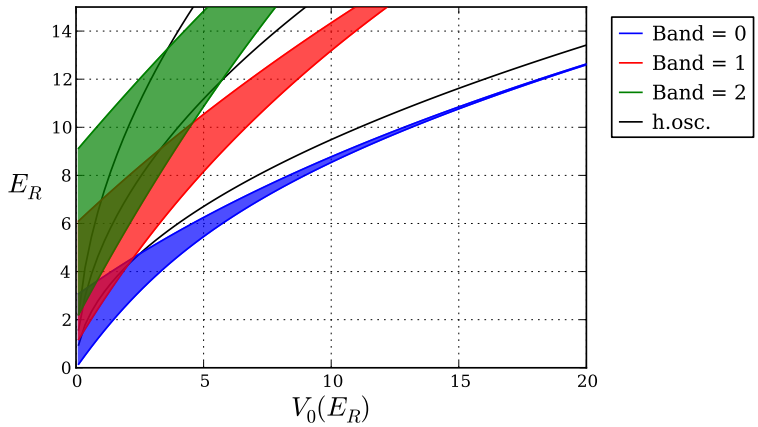

Figure 6: Band structure in a 3D optical lattice. Each band is indicated by the colored area, the harmonic oscillator states in an isolated lattice site are shown as black lines.

The Wannier states in a 3D lattice are simply products of the Wannier states in each of the three spatial coordinates. They are defined as

$$w^n(\boldsymbol{r}-\boldsymbol{r}_j)=\frac{1}{L^3}\sum_{\boldsymbol{q}}e^{-i\boldsymbol{q}\cdot\boldsymbol{r}_j}\prod_{u=x,y,z}\psi_{q_u}^{n_u}(u) \tag{14}$$

where L^3 is the total number of sites in the lattice.

3 Hubbard Hamiltonian

The hamiltonian for a single atom in a 3D optical lattice is given by

$$H_{\text{single,3D}}=-\frac{\hbar^2}{2m}\left(\frac{\partial^2}{\partial x^2}+\frac{\partial^2}{\partial y^2}+\frac{\partial^2}{\partial z^2}\right)+V_0\left(\cos^2(kx)+\cos^2(ky)+\cos^2(kz)\right) \tag{15}$$

and when N particles are considered, along with their interactions the hamiltonian takes a more complicated form

$$\begin{aligned}H=&\sum_l^N\left[-\frac{\hbar^2}{2m}\left(\frac{\partial^2}{\partial x_l^2}+\frac{\partial^2}{\partial y_l^2}+\frac{\partial^2}{\partial z_l^2}\right)+V_0\left(\cos^2(kx_l)+\cos^2(ky_l)+\cos^2(kz_l)\right)\right]\\&+\frac{1}{2}\sum_{l,m,l\neq m}^N V_{\text{int}}(\boldsymbol{r}_l,\boldsymbol{r}_m)\\=&H_0+H_{\text{int}}\end{aligned} \tag{16}$$

where the particles are labeled by indices l,m, and V_{int} is the potential energy of interaction between two partcles. In the last line we have defined the more concise notation that splits the Hamiltonian into the non-interacting (H_0) and the interacting (H_{int}) parts. Solving this problem is a daunting task primarily for two reasons:

1. The Bose or Fermi statistics of the identical particles under consideration require the wavefunctions to be symmetrized or antysymmetrized products of single-particle wavefunctions.
2. The interactions between the particles prevent a straightforward reformulation of the problem as a collection of easier-to-solve single particle hamiltonians.

The formalism of many-body theory encapsulates a series of methods to deal with the two issues mentioned above. First, the reformulation of the Schrodinger equation in the language of second quantization provides the advantage that the statistics are automatically taken into account by the notation, so one can essentially forget about the the (anti)symmetrization of the many-particle wave functions. The small price to pay is that one needs to be very careful and consistent about the order in which operators show up in the notation, since the symmetry properties of the resulting states are contained in the commutation relations defined between the operators. Furthermore, second quantization makes it easy to consider the extended Hilbert space where the number of particles is not fixed, this is known as Fock space.

For weak interactions, many-body theory provides a solution to the problem in terms of perturbation expansions for the physical quantities of interest. The theoretical formalism also reduces most of the important physical quantities in terms of certain matrix elements (Green's functions) which allows the user to concentrate on obtaining such matrix elements which serve as a starting point for the exploration of the properties of any system. The complication arises when the interactions are not weak, and the perturbative approach of the many-body formalism breaks down. For this reason, the Hubbard model with strong interactions (we will quantify the definition of strong later on) has been a major challenge for theoretical physicists over the last four decades.

3.1 Second quantization

The contents of this section follow the treatment in the books by Fetter and Walecka [5] and Schwabl [6].

Let's start with a complete orthonormal set of single particle states $\{|i\rangle\} = \{|1\rangle, |2\rangle, \ldots\}$, using these states we can write the basis states for the N-particle system as

$$|i_1, \ldots i_\alpha, \ldots i_N\rangle \tag{17}$$

which represents a state in which particle 1 is in state $i_1 \in \{|i\rangle\}$, particle α is in state i_α and so on. These product states are not eigenstates of the permutation operator P_{ij} which interchanges particles i and j. However, starting from the product states we can obtain the symmetrized (bosons) and antisymmetrized (fermions) normalized basis states.

For bosons the normalized symmetrized states are

$$|n_1, n_2, \ldots\rangle = \frac{1}{\sqrt{N! n_1! n_2! \ldots}} \sum_P P|i_1, i_2, \ldots i_N\rangle \tag{18}$$

where the sum over P runs over all $N!$ elements of the permutation group for N objects. In this expression, n_1 is the number of times that the state $|1\rangle$ occurs among the N particles, or in other words, n_1 is the number of particles in state $|1\rangle$. The sum of all occupation numbers n_i must equal the total number of particles, but otherwise there is no restriction in the occupation number for bosons.

For fermions the normalized antysymmetrized states are written in the form of Slater determinants:

$$\begin{aligned} |n_1, n_2, \ldots\rangle =& \frac{1}{\sqrt{N!}} \sum_P (-1)^P P|i_1, i_2, \ldots i_N\rangle \\ =& \frac{1}{\sqrt{N!}} \begin{vmatrix} |i_1\rangle_1 & |i_1\rangle_2 & \cdots & |i_1\rangle_N \\ \vdots & \vdots & \ddots & \vdots \\ |i_N\rangle_1 & |i_N\rangle_2 & \cdots & |i_N\rangle_N \end{vmatrix} \end{aligned} \tag{19}$$

In this case, the product states are multiplied by -1 for odd permutations, and the occupation numbers n_i can only take the values 0 or 1.

For both bosons and fermions, we can combine the states for $N = 0, 1, 2, \ldots$ particles to obtain a complete orthonormal set of states for arbitrary particle number. This set of states, which are referred to as number states, spans what is called the Fock space.

We now define the creation operators for bosons, which allow us to take a state from the subspace of N particles, to the subspace of $N + 1$ particles.

$$a_i^\dagger |\ldots, n_i, \ldots\rangle = \sqrt{n_i + 1}\,|\ldots, n_i + 1, \ldots\rangle \tag{20}$$

It follows that the adjoint of the creation operator is the annihilation operator and satisfies

$$a_i |\ldots, n_i, \ldots\rangle = \begin{cases} \sqrt{n_i}\,|\ldots, n_i - 1, \ldots\rangle & \text{if } n_i \geq 0, \\ 0 & \text{if } n_i = 0 \end{cases} \tag{21}$$

The creation and annihilation operators are defined such that one can create any state starting from the vacuum state $|0\rangle \equiv |0, 0, \ldots\rangle$ in which there are no particles at all. In more formal terms

$$|n_1, n_2, \ldots\rangle = \frac{1}{\sqrt{n_1! n_2! \ldots}} (a_1^\dagger)^{n_1} (a_2^\dagger)^{n_2} \ldots |0\rangle \tag{22}$$

The boson creation and annihilation operators satisfty the Bose communtation relations

$$[a_i, a_j] = 0 \qquad [a_i^\dagger, a_j^\dagger] = 0 \qquad [a_i, a_j^\dagger] = \delta_{ij} \tag{23}$$

In the case of fermions we want to also define creation operators such that the number states can be written as in Eq. 22. A subtlety arises in the case of fermions since the order in which the creation operators are applied affects the resulting number state[2]. Take the number state defined in Eq. 19. If we interchange the state labels 1 and 2 we get

$$\begin{aligned} |n_2, n_1, \ldots\rangle =& \frac{1}{\sqrt{N!}} \sum_P (-1)^P P |i_2, i_1, \ldots i_N\rangle \\ =& -\frac{1}{\sqrt{N!}} \sum_P (-1)^P P |i_1, i_2, \ldots i_N\rangle \\ =& -|n_1, n_2, \ldots\rangle \end{aligned} \tag{24}$$

where the minus sign in the second line is a result of the properties of determinants, namely you get a minus sign if you exchange two columns.

If we adopt as a definition of the creation operators the following expression for the number state

$$|n_1, n_2, \ldots\rangle = (a_1^\dagger)^{n_1} (a_2^\dagger)^{n_2} \ldots |0\rangle \quad , \qquad n_i = 0, 1 \tag{25}$$

then using the result of Eq. 24 above, the fermion creation operators must satisfy the following anti-commutation relation

$$a_i^\dagger a_j^\dagger + a_j^\dagger a_i^\dagger \equiv [a_i^\dagger, a_j^\dagger]_+ = 0 \tag{26}$$

Notice that this also contains the necessary implication that $(a_i^\dagger)^2 = 0$, which is a manifestation of the Pauli exclusion principle. It follows from here that the creation and annihilation operators for fermions satisfy

$$\begin{aligned} a_i^\dagger |\ldots, n_i, \ldots\rangle =& (1 - n_i)(-1)^{\sum_{k<i} n_k} |\ldots, n_i + 1, \ldots\rangle \\ a_i |\ldots, n_i, \ldots\rangle =& n_i (-1)^{\sum_{k<i} n_k} |\ldots, n_i - 1, \ldots\rangle \end{aligned} \tag{27}$$

and also that they satisfy the Fermi anticommutation relations

$$[a_i, a_j]_+ = 0 \qquad [a_i^\dagger, a_j^\dagger]_+ = 0 \qquad [a_i, a_j^\dagger]_+ = \delta_{ij} \tag{28}$$

From now on we shall focus on the case of Fermions, since this is the most relevant for our experiment.

3.2 Operators in second quantization

So far two great leaps have been taken:

1. We have swept antisymmetrization under the rug by introducing the number states, defined from the vacuum in terms of creation operators wich satisfy the Fermi anticommutation reations.
2. We started from an N particle hamiltonian, but we have now defined states that can handle the description of systems with an arbitrary number of particles

[2]This is not a problem in bosons which is seen by looking at Eq. 22 and recalling that the Bose commutation relations say that all creation operators commute

The two ideas mentioned are related to the states used to describe the system, now we will turn to the problem of the observables and see how they are handled in the second quantization.

Let us consider the following sum over particles $\sum_\alpha |i\rangle_\alpha\langle j|_\alpha$ and apply it to the number states as defined in Eq. 19

$$\left(\sum_\alpha |i\rangle_\alpha\langle j|_\alpha\right)|n_1,n_2,\ldots\rangle = \frac{1}{\sqrt{N!}}\sum_P(-1)^P P\left(\sum_\alpha |i\rangle_\alpha\langle j|_\alpha|i_1,i_2,\ldots i_N\rangle\right) \tag{29}$$

On the left hand side, for the term in parenthesis not to vanish, there must be one particle in state $|j\rangle$, so we must have $n_j = 1$ in the initial state. Also, since these are fermions, there can be no particles in state $|i\rangle$ in the intitial state, so $n_i = 0$, or else the Slater determinant operator will make the state vanish after applying the $|i\rangle\langle j|$. If the particle initially in state $|j\rangle$ is labeled as β then the two mentioned conditions can be embodied as

$$\begin{aligned}\left(\sum_\alpha |i\rangle_\alpha\langle j|_\alpha\right)|n_1,n_2,\ldots\rangle =& n_j(1-n_i)\frac{1}{\sqrt{N!}}\sum_P(-1)^P P\left(|i\rangle_\beta \underbrace{|i_1,i_2,\ldots i_N\rangle}_{\text{wihtout } |j\rangle_\beta}\right)\\ =& n_j(1-n_i)\frac{1}{\sqrt{N!}}\begin{vmatrix} |i_1\rangle_1 & |i_1\rangle_2 & \cdots & |i_1\rangle_N \\ \vdots & \vdots & & \vdots \\ |i\rangle_1 & |i\rangle_2 & \cdots & |i\rangle_N \\ \vdots & \vdots & & \vdots \\ |i_N\rangle_1 & |i_N\rangle_2 & \cdots & |i_N\rangle_N \end{vmatrix}\end{aligned} \tag{30}$$

In the determinant of the left the state $|i\rangle$ appears in the j^{th} row, so a few rows need to be exchanged to put it in the correct place according to our sign convention for the number states.

$$\begin{aligned}\left(\sum_\alpha |i\rangle_\alpha\langle j|_\alpha\right)|n_1,n_2,\ldots\rangle =& n_j(1-n_i)|\ldots,n_i+1,\ldots,n_j-1,\ldots\rangle \times \begin{cases}(-1)^{\sum_{k<j}n_k+\sum_{k<i}n_k} & \text{if } i\le j,\\ (-1)^{\sum_{k<j}n_k+\sum_{k<i}n_k-1} & \text{if } i>j\end{cases}\\ =& a_i^\dagger a_j|n_1,n_2,\ldots\rangle\end{aligned} \tag{31}$$

where the last equality can be obtained by examining the definition of the creating and annihilation operators given above.

After this last step we can establish the important relation

$$\sum_\alpha |i\rangle_\alpha\langle j|_\alpha = a_i^\dagger a_j \tag{32}$$

We now turn our attention to the operators in the N-particle system. Consider an operator T that is a sum over single particle operators

$$T = \sum_\alpha t_\alpha \tag{33}$$

If we insert the completness relation for the single particle states twice in this sum we have

$$\begin{aligned}T =& \sum_\alpha\left(\sum_i |i\rangle_\alpha\langle i|_\alpha\right)t_\alpha\left(\sum_j |j\rangle_\alpha\langle j|_\alpha\right)\\ =& \sum_{ij}\langle i|t|j\rangle\sum_\alpha |i\rangle_\alpha\langle j|_\alpha\\ =& \sum_{ij}\langle i|t|j\rangle a_i^\dagger a_j \equiv \sum_{ij} t_{ij}a_i^\dagger a_j\end{aligned} \tag{34}$$

This is the other big leap provided by the second quantization: the operators which were written as a sum over particles now are written as a sum of creation and annihilation operators over single particle states.

Operators like the potential energy, which are a sum over two-particle (or many-particle) operators, can be equally expressed as sums of creation and annihilation operators. For a two-body operator we have the expression

$$\begin{aligned} F =& \frac{1}{2}\sum_{\alpha\neq\beta} f(\boldsymbol{r}_\alpha, \boldsymbol{r}_\beta) \\ =& \frac{1}{2}\sum_{ijkm} \langle ij|f|km\rangle a_i^\dagger a_j^\dagger a_m a_k \end{aligned} \tag{35}$$

3.3 Second quantized Hubbard hamiltonian

The Hubbard hamiltonian in Eq. 16 is a sum of two single-particle operators and one two-particle operator. These are respectively: the kinetic energy, the energy of the atoms in the lattice potential, and the interactions between the atoms. As a single-particle basis we pick the Wannier states that were derived in Section. 1.3

In the Hubbard hamiltonian the two single-particle operators are grouped together to define the non-interacting part of the hamiltonian

$$\begin{aligned} H_0 =& \sum_l^N -\frac{\hbar^2}{2m}\left(\frac{\partial^2}{\partial x_l^2}+\frac{\partial^2}{\partial y_l^2}+\frac{\partial^2}{\partial z_l^2}\right) + V_0\left(\cos^2(kx_l)+\cos^2(ky_l)+\cos^2(kz_l)\right) \\ =& \sum_l^N H^l_{\text{single,3D}} \end{aligned} \tag{36}$$

3.3.1 Tunneling matrix element, t

H_0 is a single particle operator, so it's second quantized form is

$$\begin{aligned} H_0 =& \sum_{ij} \langle i|H_{\text{single,3D}}|j\rangle a_i^\dagger a_j \\ =& -\sum_{ij} t_{ij} a_i^\dagger a_j \end{aligned} \tag{37}$$

Note that the sign of t_{ij} was picked rather arbitrarily to follow the usual conventions. We now proceed to find the value of the matrix element. We use the definition of the Wannier states given in Eq. 14 to find

$$\begin{aligned} -t_{ij} =& \frac{1}{L^6}\int \mathrm{d}\boldsymbol{r}\ \sum_{\boldsymbol{q}'} e^{i\boldsymbol{q}'\cdot\boldsymbol{r}_i} \prod_{u'=x,y,z} \psi_{q'_{u'}}^{n'_{u'}*}(u')\Big(H_{\text{single,3D}}\Big)\sum_{\boldsymbol{q}} e^{-i\boldsymbol{q}\cdot\boldsymbol{r}_j}\prod_{u=x,y,z}\psi_{q_u}^{n_u}(u) \\ =& \sum_{\boldsymbol{q}\boldsymbol{q}'}\frac{E^n_{\boldsymbol{q}}}{L^6} e^{i\boldsymbol{q}'\cdot\boldsymbol{r}_i}e^{-i\boldsymbol{q}\cdot\boldsymbol{r}_j}\int \mathrm{d}\boldsymbol{r}\prod_{u'=x,y,z}\psi_{q'_{u'}}^{n'_{u'}*}(u')\prod_{u=x,y,z}\psi_{q_u}^{n_u}(u) \\ =& \sum_{\boldsymbol{q}\boldsymbol{q}'}\frac{E^n_{\boldsymbol{q}}}{L^6} e^{i\boldsymbol{q}'\cdot\boldsymbol{r}_i}e^{-i\boldsymbol{q}\cdot\boldsymbol{r}_j}\delta_{\boldsymbol{q}\boldsymbol{q}'}\delta_{nn'}L^3 \\ =& \frac{1}{L^3}\sum_{\boldsymbol{q}} E^n_{\boldsymbol{q}} e^{i\boldsymbol{q}\cdot(\boldsymbol{r}_i-\boldsymbol{r}_j)} \end{aligned} \tag{38}$$

We observe that there is no amplitude to go between states that are in two different bands, as is indicated by the appereance of $\delta_{nn'}$. In what follows we will consider only the lowesrt band, $n = 0$, so we will drop the band index altogether. This simplification imposes two important requirements for our system:

1. The temperature and the Fermi energy need to be small compared to the energy gap between the lowest and first excited band.
2. The interaction energy scale must also be small comapred to the energy gap between the lowest and first excited band.

In the 3D lattice, the energy $E_{\boldsymbol{q}} = \sum_{u=x,y,z} E^u_{q_u}$, and by inserting this into the sum for t_{ij} above we find

$$-t_{ij} = \frac{1}{L^3}\left[\left(\sum_{q_x} E^{\mathrm{1D}}_{q_x} e^{iq_x x_{ij}}\right)\sum_{q_y} e^{iq_y y_{ij}} \sum_{q_z} e^{iq_z z_{ij}} + \sum_{q_x} e^{iq_x x_{ij}}\left(\sum_{q_y} E^{\mathrm{1D}}_{q_y} e^{iq_y x_{ij}}\right)\sum_{q_z} e^{iq_z z_{ij}} + \sum_{q_x} e^{iq_x x_{ij}} \sum_{q_y} e^{iq_y y_{ij}}\left(\sum_{q_z} E^{\mathrm{1D}}_{q_z} e^{iq_z z_{ij}}\right)\right] \tag{39}$$

We make use of the identity $\sum_{q_x} e^{iq_x(x_i - x_j)} = L\delta_{x_i x_j}$, and similarly for y, z to obtain

$$-t_{ij} = \frac{1}{L}\left[\left(\sum_{q_x} E^{\mathrm{1D}}_{q_x} e^{iq_x x_{ij}}\right)\delta_{y_i y_j}\delta_{z_i z_j} + \left(\sum_{q_y} E^{\mathrm{1D}}_{q_y} e^{iq_y x_{ij}}\right)\delta_{x_i x_j}\delta_{z_i z_j} + \left(\sum_{q_z} E^{\mathrm{1D}}_{q_z} e^{iq_z z_{ij}}\right)\delta_{x_i x_j}\delta_{y_i y_j}\right] \tag{40}$$

We see that if $i = j$ we have

$$-t_{ii} = \frac{3}{L}\sum_q E^{\mathrm{1D}}_q \tag{41}$$

This term just adds an overall energy (proportional to the number of particles in the system) to the hamiltonian, so we just ignore it for convenience. If on the other hand $i \neq j$, then we see that we can only consider the posibility that one of the x_{ij}, y_{ij}, z_{ij} is non-zero, otherwise all three of the terms in the expression above will vanish due to the Kronnecer delta terms. The expression for the tunneling matrix elements simplifies to

$$t_{ij} = -\frac{1}{L}\sum_q E^{\mathrm{1D}}_q e^{iq\Delta_{ij}} \tag{42}$$

where Δ_{ij} is the distance between sites at $\boldsymbol{r}_i$ and $\boldsymbol{r}_j$, and r_{ij} must be purely directed along x, y, or z. Also, as in the definition of the 1D Wannier states, the sum over q runs over the discrete values $q = \frac{2\pi n}{a}\ \forall n \in \{0, 1, \ldots L-1\}$

We point out here that the tunneling matrix element can be computed directly from the integral

$$-t_{ij} = \int \mathrm{d}\boldsymbol{r}\, w_i(\boldsymbol{r}) H_{\mathrm{single,3D}} w_j(\boldsymbol{r}) \tag{43}$$

Numerical forms of the Wannier functions and their derivatives are easily obtained from the formulas in Sec. 1.3. Calculating the tunneling matrix element from the Wannier functions is computationally more expensive than obtaining it as a sum over the energy eigenvalues.

We observe from Eq. 42 that t_{ij} and E^{1D}_q are the Fourier series of one another, or in other words that the relation just shown can be inverted to obtain

$$E^{\mathrm{1D}}_q = -\sum_{\Delta_{ij}} t_{ij} e^{-iq\Delta_{ij}} \tag{44}$$

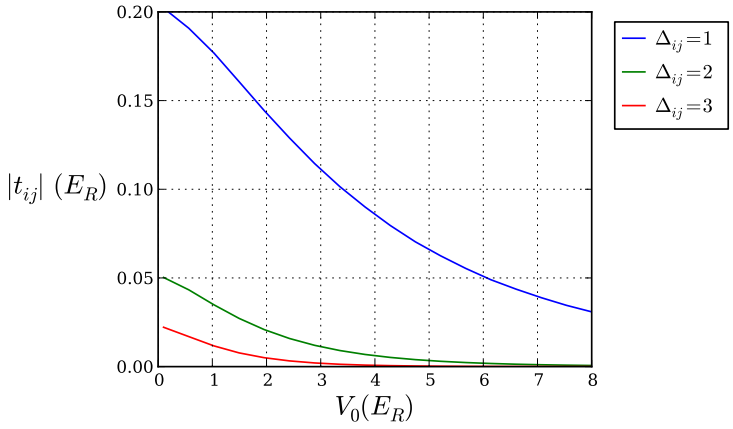

Figure 7: Tunneling matrix element in an optical lattice as a function of lattice depth. Nearest-neighbor and beyond nearest neighbor matrix elements are shown to illustrate the range of lattice depths for which the tight-binding limit is a good approximation. X_{ij} corresponds to the distance between intial and final site in the tunneling matrix element.

In the tight-binding approximation terms for which i, j are not nearest neighbors are neglected, and Δ_{ij} can only take the values $\{-a, a\}$. In this case we use $t_{ij} \equiv t$, and t satisfies

$$E^{\mathrm{1D}}_{q,\mathrm{tb}} = -2t\cos(qa) \tag{45}$$

This gives an expression that relates the bandwidth, W_{1D}, of the 1D lattice to the tunneling matrix element t

$$W_{\mathrm{1D}} = 4t. \tag{46}$$

In 3D this becomes $W_{\mathrm{3D}} = 12t$.

It is useful to find out the range of lattice depths for which the tight-binding approximation is valid in the optical lattice potential. To do this we just need to look at the tunneling matrix elements for beyond nearest-neighbor tunneling, this is shown in Fig. 7, which shows that for lattice depths $\gtrsim 5E_R$ we can safely ignore tunneling beyond nearest neighbors.

Another way of estimating the tunneling matrix element, suggested in [7], is by using the relationship $t = W_{\mathrm{1D}}/4$, valid in the tight-binding limit, and obtaining the bandwidth from the Mathieu functions, which are solutions to the Schrodinger equation in a 1D lattice. This yields the result

$$t \simeq \frac{4}{\sqrt{\pi}} V_0^{3/4} \exp(-2\sqrt{V_0}) \tag{47}$$

where t and V_0 are in units of the recoil energy. The comparision between the result from Eq. 42 and the result from the Mathieu functions is shown in Fig. 8.

Finally, we have the second quantized form of H_0 in the tight-binding limit

$$H_0 = -t \sum_{\langle ij \rangle} a_i^\dagger a_j \tag{48}$$

where the $\langle\rangle$ denote nearest-neighbors, and the creation operator $a_i^\dagger$ create particles in the Wannier state localized at site i.

Notice that up to now we have ignored the spin part of the wavefunction. We can include it easilly by noticing that H_0 does not act on the spin at all, so the states $|i\rangle$ and $|j\rangle$ that we have used in the

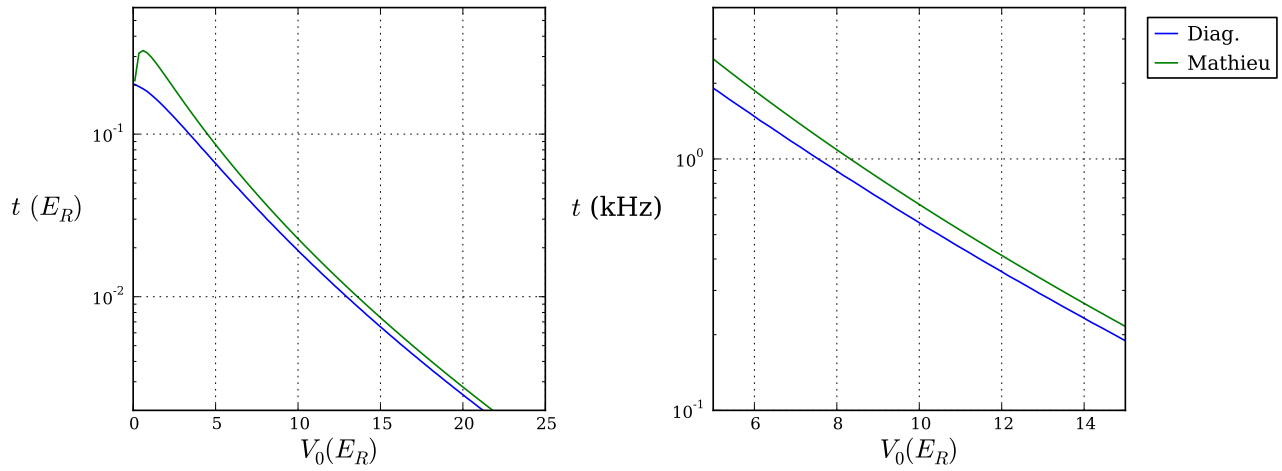

Figure 8: Nearest neighbor tunneling matrix element in an optical lattice as a function of lattice depth. Comparison between the result from Eq. 42 and the one obtained from the Mathieu functions. The right panel shows the tunneling rate in kHz for the mass of a ^{6}Li atom.

derivation above need to have the same spin. With the spin included, our basis set is now larger which can be taken care of by including a sum over spin states.

$$H_0 = -t \sum_{\langle ij\rangle,\sigma=\uparrow\downarrow} a^\dagger_{i\sigma} a_{j\sigma} \tag{49}$$

3.3.2 On-site interaction energy, U

The interaction part of the hamiltonian for N particles in a 3D lattice is given by

$$H_{\text{int}} = \frac{1}{2} \sum_{l,m,l\neq m}^{N} V_{\text{int}}(\boldsymbol{r}_l, \boldsymbol{r}_m) \tag{50}$$

This is a two-particle operator, and its second quantized form is given by

$$H_{\text{int}} = \frac{1}{2} \sum_{i,j,k,m} \langle ij|V_{\text{int}}|km\rangle a^\dagger_i a^\dagger_j a_m a_k \tag{51}$$

where

$$\langle ij|V_{\text{int}}|km\rangle = \int \mathrm{d}\boldsymbol{r} \int \mathrm{d}\boldsymbol{y} \;\; \varphi^*_i(\boldsymbol{r})\varphi^*_j(\boldsymbol{y}) V_{\text{int}}(\boldsymbol{r},\boldsymbol{y})\varphi_k(\boldsymbol{r})\varphi_m(\boldsymbol{y}) \tag{52}$$

The interaction between ultracold atoms can be described in terms of the s-wave scattering length, a, and a pseudopotential given by [7]

$$V(x,y) = \frac{4\pi\hbar^2 a}{m} \delta(\boldsymbol{r}-\boldsymbol{y}) \tag{53}$$

so the matrix element above can be written as

$$\langle ij|V_{\text{int}}|km\rangle = \frac{4\pi\hbar^2 a}{m} \int \mathrm{d}\boldsymbol{r} \;\; \varphi^*_i(\boldsymbol{r})\varphi^*_j(\boldsymbol{r})\varphi_k(\boldsymbol{r})\varphi_m(\boldsymbol{r}) \tag{54}$$

Our basis states, φ, are the 3D Wannier states defined in Eq. 14, which are separable in the three spatial coordinates. We recall that the Wannier states are labeled by the lattice site on which they are centerend and by their band index. If we explicitly write out the two labels in the expression above we obtain

$$\langle ij|V_{\text{int}}|km\rangle = \frac{4\pi\hbar^2 a}{m} \prod_{v=x,y,z} \int \mathrm{d}v \;\; w_i^{n_i}(v) w_j^{n_j}(v) w_k^{n_k}(v) w_m^{n_m}(v) \tag{55}$$

The Wannier function along x, y, z depends on the lattice depth along the respective coordinate. We will consider a lattice with different depths along the three spatial coordinates, $\boldsymbol{V}_0 = (V_{0x}, V_{0y}, V_{0z})$. At this point we make the approximation of neglecting all of the off-site interaction terms, which can be justified by the localized nature of the Wannier states. Furthermore, we consider only Wannier states in the lowest band, which is valid for scattering lengths smaller than the single-site harmonic oscillator length [8]. With this considerations, and also explicitly writing down the spin quantum number, which so far was implicit in the indices $ijkm$, we find

$$\begin{aligned} H_{\text{int}} =& \frac{U}{2} \sum_{\sigma\neq\sigma'} \sum_i a_{i\sigma}^\dagger a_{i\sigma'}^\dagger a_{i\sigma'} a_{i\sigma} \\ =& \frac{U}{2} \sum_{\sigma\neq\sigma'} \sum_i n_{i\sigma'} n_{i\sigma} \\ =& U \sum_i n_{i\uparrow} n_{i\downarrow} \end{aligned} \tag{56}$$

where now i is an index that runs over lattice sites, and

$$U = \frac{4\pi\hbar^2 a}{m} \prod_{v=x,y,z} \int w(v)^4 \mathrm{d}v \tag{57}$$

In units of E_R, and keeping in mind that we defined the lattice spacing as unity

$$U = \frac{8}{\pi} a_s \prod_{v=x,y,z} \int w(v)^4 \mathrm{d}v \tag{58}$$

where now the scattering length a_s must be in units of the lattice spacing.

If the Wannier state is approximated by the Gaussian ground state in the local oscillator potential of one lattice site, the integral can be carried out explicity and one gets [7]

$$U = \sqrt{8\pi} a_s V_0^{3/4} \tag{59}$$

where, again, the scattering length must be in units of the lattice spacing.

Alternatively we can use the Wannier states which were calculated in Sec. 1.3 and obtain a more accurate result. Figure 9 shows a comparison of the two methods for a lattice with $\lambda = 1064\,\text{nm}$.

If the scattering length is too large, and the on-site interaction term calculated here starts being comparable to the interband spacing then the single band approximation that we introduced is no longer valid. One can treat the problem of two atoms intearcting in the local harmonic oscillator around a lattice site [8]. Another approach consists of redefining the single particle basis states (using linear combinations of Wannier states in different bands) such that the interaction matrix element is diagonal in the new basis, see for instance [9, 10].

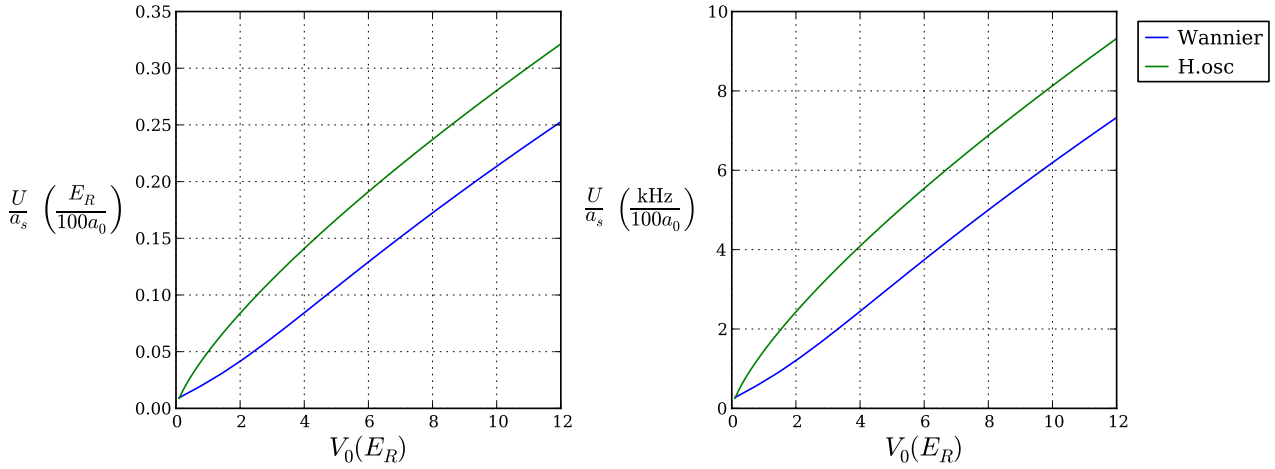

Figure 9: On-site interactions in a 3D lattice as a function of lattice depth. Numerical calculation using Wannier functions compeared to the approximation using harmonic oscillator states. The lattice depth is the same in all three directions of the lattice. The lattice wavelength is 1064 nm, and it is used to express the interactions in units of recoils divided by Bohr radius. The right panel shows it in kHz over Bohr radius for the mas of a ^{6}Li atom.

4 High-temperature series expansion for the single band Hubbard model

In the atomic limit, where tunneling between sites is neglected completely, the Hubbard model can solved exactly. In this case the tunneling part of the hamiltonian can be treated as a perturbation and we can gain insight in to the different phases that the system can exhibit. This Section follows the treatment that can be found in [11, 9].

We work in the grand canonical ensemble, so we include a global chemical potential in the hamiltonian

$$\begin{aligned} H =& \left(U \sum_i n_{i\uparrow} n_{i\downarrow} - \mu \sum_i (n_{i\uparrow} + n_{i\downarrow}) \right) - t \sum_{\langle ij \rangle, \sigma} a^\dagger_{i\sigma} a_{j\sigma} \\ =& H_0 + H_1 \end{aligned} \tag{60}$$

For the unberturbed part, H_0, the grand canonical partition function is

$$Z_0 = \text{Tr} e^{-\beta H_0} \tag{61}$$

Since the unperturbed part is a sum over sites, the partition function becomes a product of the single site partition function, $Z_0 = z_0^k$, for a system with k sites. The single site partition function is easy to calculate because the trace runs over the only four possible states in a single site $\{|0\rangle, |\uparrow\rangle, |\downarrow\rangle, |\uparrow\downarrow\rangle\}$.

$$z_0 = 1 + 2e^{\beta\mu} + e^{\beta(2\mu - U)} = 1 + 2z + z^2 u \tag{62}$$

where we have defined $z = e^{\beta\mu}$ and $u = e^{-\beta U}$. Among the relevant physical quantities that can be obtained are the number of particles, the number of double occupancies, and the entropy per site. These are obtained from the first derivatives of the grand canonical potential, Ω

$$\Omega = -\frac{\ln Z}{\beta} \tag{63}$$

$$N = -\frac{\partial \Omega}{\partial \mu} \tag{64}$$

$$D = \frac{\partial \Omega}{\partial U} \tag{65}$$

$$S = -\frac{\partial \Omega}{\partial T} \tag{66}$$

Also, from the second derivatives of the grand potential one can obtain the fluctuations in any of these quantitites.

For the full hamiltonian the grand canonical partition function Z can be expanded in a perturbation series [11]

$$\begin{aligned} Z =& \mathrm{Tr} e^{-\beta H} \\ =& Z_0 \left[1 + \sum_{n=1}^{\infty} (-1)^n \int_0^{\beta} d\tau_1 \int_0^{\tau_1} d\tau_2 \cdots \int_0^{\tau_{n-1}} d\tau_n \langle \tilde{H}_1(\tau_1) \tilde{H}_2(\tau_2) \cdots \tilde{H}_n(\tau_n) \rangle \right] \end{aligned} \tag{67}$$

where the thermal expectation value is taken with the unperturbed part of the hamiltonian

$$\langle A \rangle = \mathrm{Tr}(e^{\beta H_0} A)/Z_0 \tag{68}$$

and the tilde means that the operator is evaluated in the interaction picture for the imaginary time in parenthesis:

$$\tilde{H}_1(\tau) = e^{\tau H_0} H_1 e^{-\tau H_0} \tag{69}$$

Given the series expansion for Z, the grand potential is

$$-\beta \Omega = Z_0 + \sum_{n=1}^{\infty} (-1)^n \int_0^{\beta} d\tau_1 \int_0^{\tau_1} d\tau_2 \cdots \int_0^{\tau_{n-1}} d\tau_n \langle \tilde{H}_1(\tau_1) \tilde{H}_2(\tau_2) \cdots \tilde{H}_n(\tau_n) \rangle \tag{70}$$

One can see that the n^{th} term in the expansion has n copies of the tunneling part of the hamiltonian. Each application of H_1 in the thermal average results in a particle tunneling to a neighboring site, so we see that there will be a contribution to the expansion only if after n tunneling events all the particles come back to their original sites. A direct consequence of this is that the first order term in the expansion vanishes. The second order in the expansion corresponds to particles tunneling one site over and then coming back. Higher order terms can be represented by diagrams, to make them easier to keep track off. The contribution from orders up to $n = 9$ is shown in [11]. Here we will use up to the second order term to illustrate the phases that appear in the system.

The grand potential to second order is [11, 9]

$$-\beta \Omega_2 = k \ln z_0 + k \left(\frac{\beta t}{z_0} \right)^2 m \left(z + z^3 u + 2 z^2 \frac{1-u}{\beta U} \right) \tag{71}$$

where m is the number of nearest neighbors for each lattice site, which in the simple cubic case is $m = 6$. We see that the grand potential is proportional to the number of lattice sites, so we will obtain all the thermodynamic quantities per lattice site.

The resulting phase diagram is shown in Fig. 10. NOTE FOR GROUP MEETING: I intend to write some text that discusses the relevant phases in this phase diagram. I will discuss them in the presentation in the group meeting and add the explanatory text in this document later on.

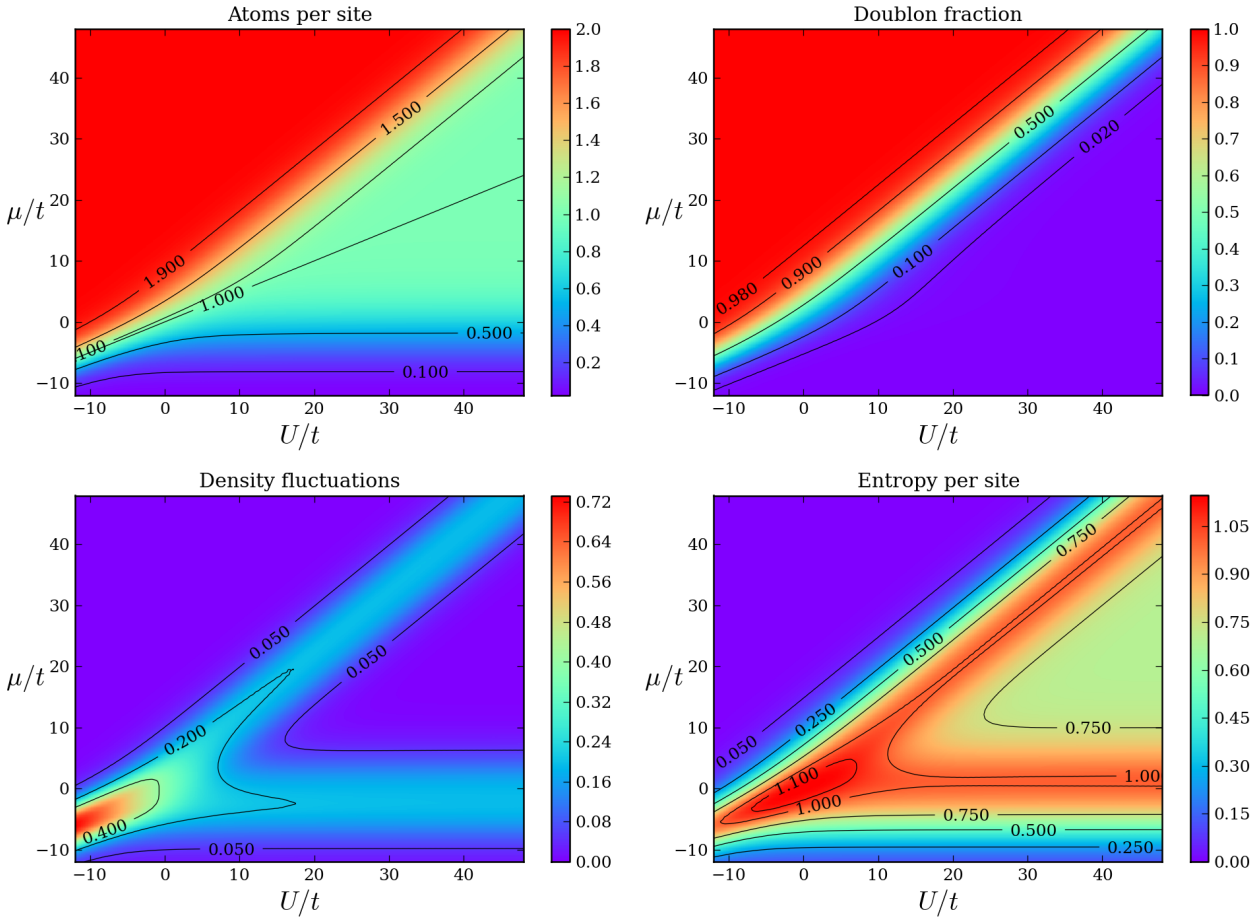

Figure 10: High temperature phase diagram of the Fermi-Hubbard model calculated using only the second order in the perturbation series.

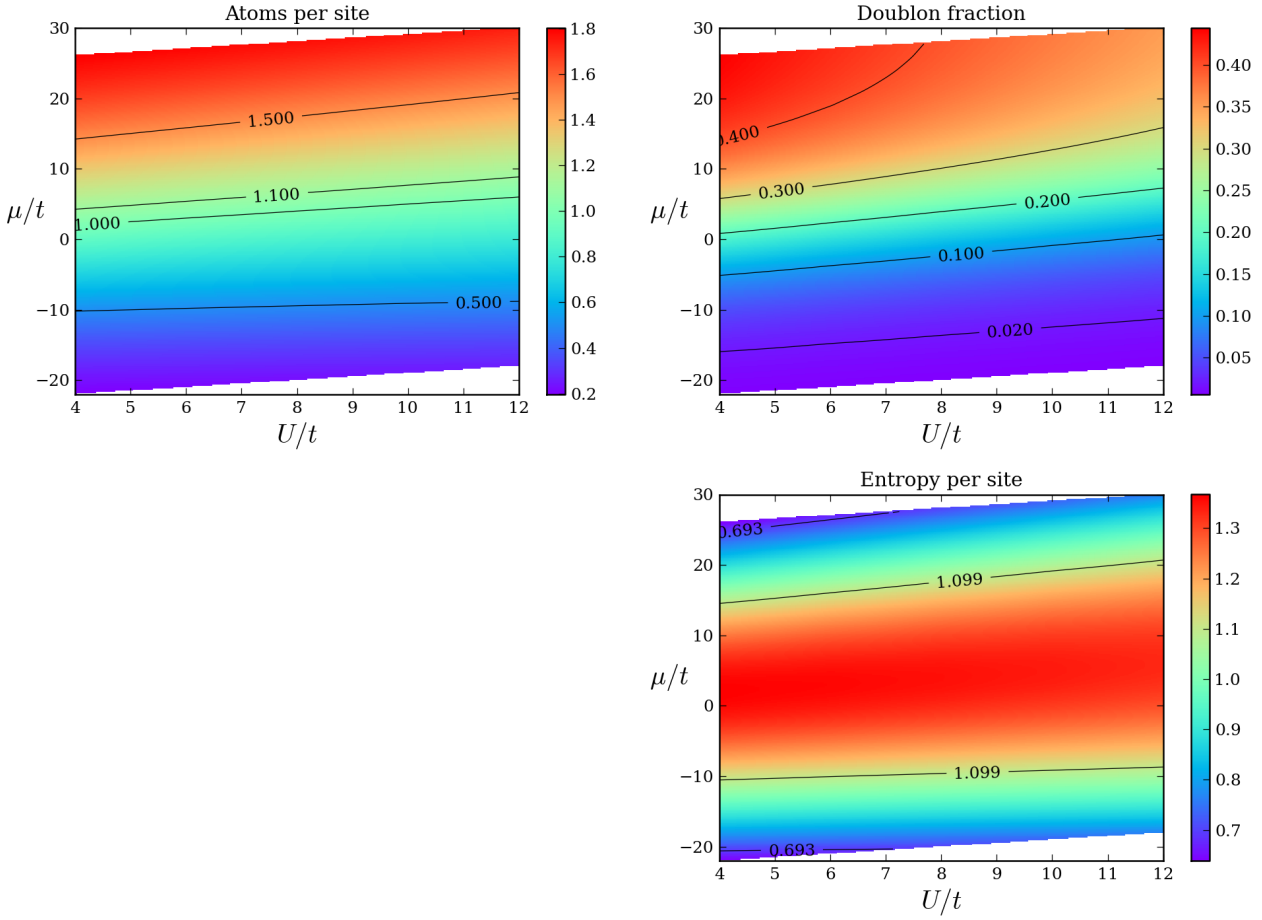

Figure 11: From [12]

4.1 Thermodynamics at colder temperatures, apparoach to the Néel transition

In this section we show the phase diagram for the Fermi-Hubbard model at lower temperatures, which are beyond the scope of the perturbation expansion shown in the previous section. The phase diagram was calculated in [12] by using cluster dynamical mean-field theory, and they have made their results available in the supplementary material accompanying their paper. In Figures **??** we show the resulting phase diagram for $T/t = 10$, 1, and 0.3 respectively.

5 Local density approximation

The phase diagrams calculated in the two previous sections assume a homogeneous lattice. In our experiment the lattice has an underlying confining potential, which can be dealt with by considering a local chemical potential at each point in the trap given by

$$\mu(\boldsymbol{r}) = \mu - V(\boldsymbol{r}) \tag{72}$$

An homogeneous lattice phase diagram can be used to obtain the local density, local entropy, and local double occupancy at any point in our system by using as inputs the local chemical potential, the local value of the tunneling matrix element and the local value of the on-site interaction.

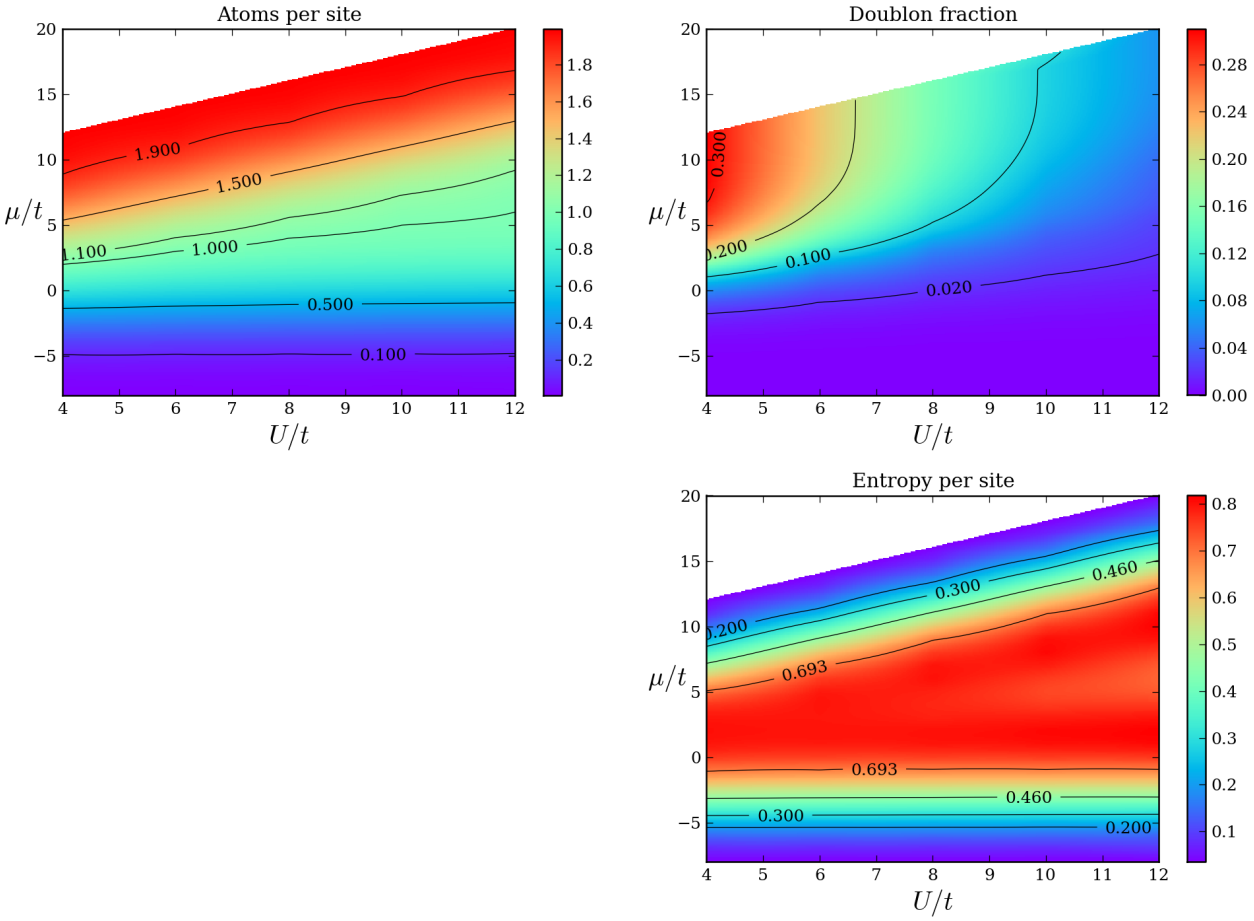

Figure 12: From [12]

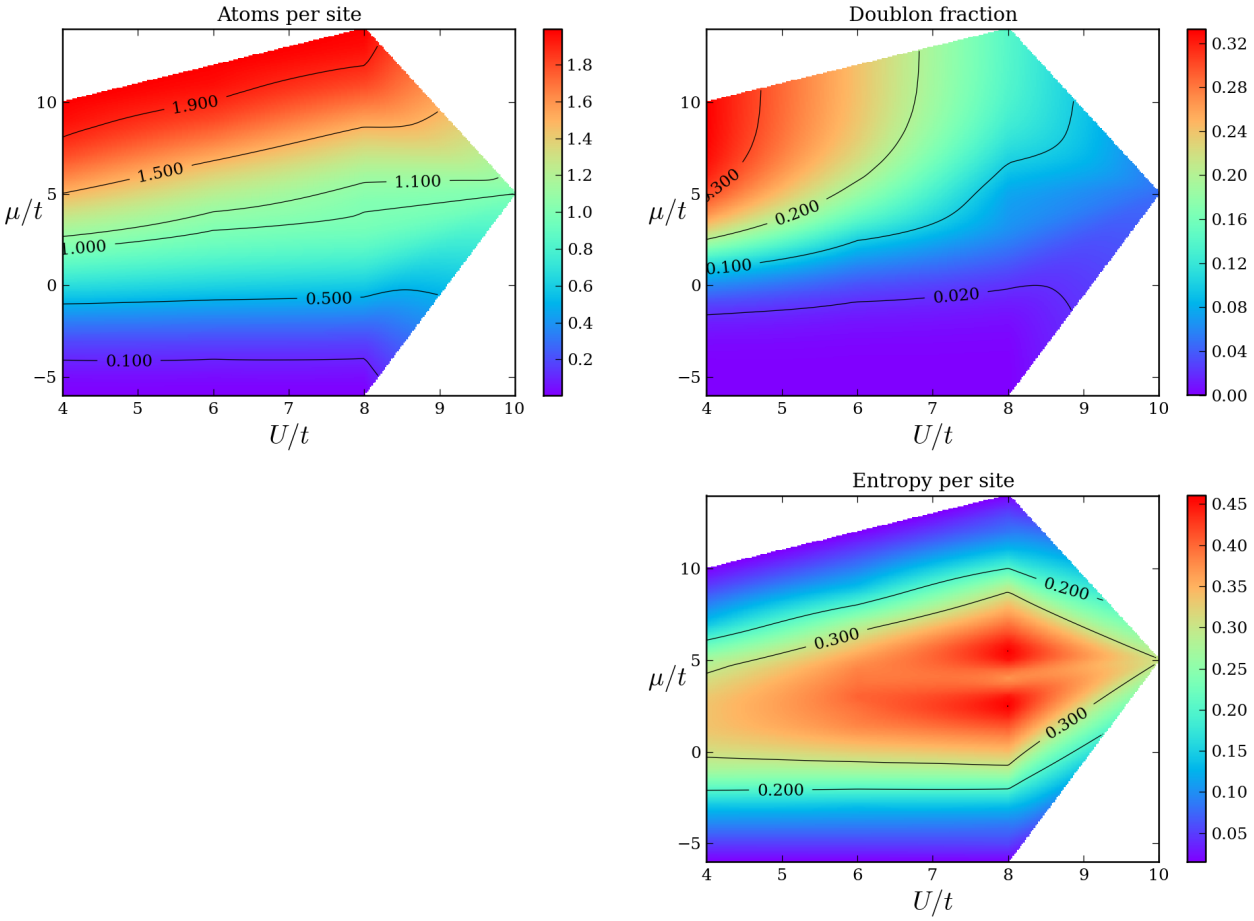

Figure 13: From [12]

The methods used to calculate the phase diagrams are related to the validity of the local density approximation. We recall that in the high temperature series expansion, the n^{th} term corresponds to a particle staring at a certain site, tunneling n times and then coming back to its original site. If $\sqrt{n}$ becomes comparable to the lenght scale of variations in the confining potential, then the local density would not be a suitable description of the system, because in those n steps the particle can sample a very different confining potential.

Similarly, in the cluster dynamical mean-field theory, results are obtained for finite sized clusters of various sizes and then extrapolated to the infinite size limit [12]. At low temperatures, the system develops long-range correlations, so large clusters are required to approximate the system. If the local site energy varies considerably over the size of a cluster then the local density approximation will break down.

5.1 Compensated lattice geometry

[13]

References

[1] O. Morsch and M. Oberthaler, "Dynamics of Bose-Einstein condensates in optical lattices," Rev. Mod. Phys. **78,** 179–215 (2006).

[2] J. C. Slater, "A Soluble Problem in Energy Bands," Phys. Rev. **87,** 807–835 (1952).

[3] C. Salomon, G. Shlyapnikov, and L. Cugliandolo, *Many-Body Physics with Ultracold Gases: Lecture Notes of the Les Houches Summer School: Volume 94, July 2010*, *Lecture Notes of the Les Houches Summer School* (OUP Oxford, 2013).

[4] W. Kohn, "Analytic Properties of Bloch Waves and Wannier Functions," Physical Review **115,** 809–821 (1959).

[5] A. Fetter and J. Walecka, *Quantum Theory of Many-particle Systems*, *Dover Books on Physics* (Dover Publications, 2003).

[6] F. Schwabl, *Advanced Quantum Mechanics*, *Advanced texts in physics* (Springer, 2005).

[7] I. Bloch and W. Zwerger, "Many-body physics with ultracold gases," Reviews of Modern Physics **80,** 885–964 (2008).

[8] T. Busch, B. Englert, K. Rzaewski, and M. Wilkens, "Two cold atoms in a harmonic trap," Foundations of Physics pp. 549–559 (1998).

[9] R. Jördens, Ph.D. thesis, ETH Zürich, 2010.

[10] M. Mark, Ph.D. thesis, Innsbruck, 2012.

[11] J. Henderson, J. Oitmaa, and M. Ashley, "High-temperature expansion for the single-band Hubbard model," Physical Review B **46,** 6328–6337 (1992).

[12] S. Fuchs, E. Gull, L. Pollet, E. Burovski, E. Kozik, T. Pruschke, and M. Troyer, "Thermodynamics of the 3D Hubbard Model on Approaching the Néel Transition," Physical Review Letters **106,** 030401 (2011).

[13] C. J. M. Mathy, D. A. Huse, and R. G. Hulet, "Enlarging and cooling the Néel state in an optical lattice," Phys. Rev. A **86,** 023606 (2012).